

## About a Novel Production Method for N-Doped Magnetic Nanocore Nanoparticles of Titania by Means of a Spinning Disk Reactor

Marco Stoller\*<sup>a</sup>, Srikanth Vuppala<sup>b</sup>, Mariantonietta Matarangolo<sup>c</sup>, Vincenzo Vaiano<sup>c</sup>, Diana Sannino<sup>c</sup>, Angelo Chianese<sup>a</sup>, Claudio Cianfrini<sup>b</sup>

<sup>a</sup> Sapienza University of Rome, Dept. of Chemical Engineering Materials Environment, Via Eudossiana 18, Rome, Italy

<sup>b</sup> Sapienza University of Rome, Dept. of Astronautics Electrical and Energy Engineering, Via Eudossiana 18, Rome, Italy

<sup>c</sup> University of Salerno, Dept. of Industrial Engineering, Via Giovanni Paolo II 132, 84084 Fisciano(SA), Italy

[marco.stoller@uniroma1.it](mailto:marco.stoller@uniroma1.it)

This study reports a novel approach to produce nitrogen doped magnetic core TiO<sub>2</sub> nanoparticles (N-TiO<sub>2</sub>/FM). The treatment of wastewater streams by photocatalysis appears a feasible pre-treatment for many subsequent purification steps, such as membranes. In order to keep high efficiencies in dealing with the wastewater streams, the photocatalyst requires to be suspended in order to reach the water surface for proper irradiation and operation. A main drawback is the recovery of the suspended photocatalyst, that may be accomplished by magnetic filters (up to 99.9%) as soon as the titania nanoparticles are attached to magnetic nanocores (FM). Moreover, the photocatalyst should react to visible light and not only to UV (as pure titania), to operate with a high energy efficient process that may use LED lamps instead of UV lamps. This property can be acquired through nitrogen doping. Therefore, the production of NMTNP may represent a general solution to all these problems. The N-TiO<sub>2</sub>/FM were synthesised starting with the production of magnetic nanocores by SDR and their coating of silica by using the Stroeber method. Finally, FM particles were dispersed in Urea solution and then titanium tetraisopropoxide (TTIP) is added to produce N-TiO<sub>2</sub>/FM, respectively. In the final stage of production, the N-TiO<sub>2</sub>/FM solution is washed and calcinated at higher temperatures. The final product is a core-shell-shell nanoparticle of FM/silica and titania. The experimental runs performed in an aerated photoreactor for phenol degradation shows the efficiency of NMTNP for purification purposes and its easily recovery by magnets.

### 1. Introduction

Water pollution has become a major problem in recent year (Muradova et al. 2016; Vilardi and Di Palma 2016). Phenolic compounds represent a threat to the environmental point of view because of their toxicity, bioaccumulation, and persistency in the environment. These materials were recorded by The Agency for Toxic Substances and Disease Registry-USA (ATSDR) as one of the year 2007 priority contaminants that have critical potential danger to human wellbeing (Shawabkeh et al. 2010; Vaiano et al., 2016). The effluents of various industries such as petrochemical, coal, pharmaceutical, wood, paint, pulp and paper industries contains phenol and its derivatives besides inorganic pollutants (Vilardi et al., 2017). Traditional techniques such as active carbon adsorption, chemical oxidation, and biological digestion have low efficiency in the removal of phenol (Stoller et al. 2016). Advanced oxidation process (AOPs) is an interesting alternative to the traditional technologies. Among AOPs, heterogeneous photocatalysis with nanoparticles have shown high efficiency in the removal of a wide range of organic contaminants, also present in low amount in wastewater (Bavasso et al. 2016). Titanium dioxide exists primarily as anatase, rutile and brookite. In comparison to rutile and brookite, the anatase phase is catalytically more active (Choquette-Labbé, Shewa, Lalman, & Shanmugam, 2014). Fujishima and Honda demonstrated the potential of titanium dioxide (TiO<sub>2</sub>) semiconductor materials to split water into hydrogen and oxygen in a photo-electrochemical cell. Their work

triggered the development of semiconductor photocatalysis for a wide range of environmental and energy applications. In the case of anatase  $\text{TiO}_2$ , the band gap is 3.2 eV, therefore UV light ( $\leq 387$  nm) is required. Later, Asahi and co-workers explored for first time the visible light activity of N-doped  $\text{TiO}_2$  produced by sputter deposition of  $\text{TiO}_2$  under an  $\text{N}_2/\text{Ar}$  atmosphere, followed by annealing under  $\text{N}_2$ . N-doped  $\text{TiO}_2$  is used to extend the photocatalyst's response into the visible region and hence improve the oxidation of several organic compounds such as chloroform, toluene, benzene, alcohols and ethers (Ruzmanova et al. 2015; Shawabkeh et al. 2010). Simultaneous  $\text{TiO}_2$  growth and N doping is achieved by hydrolysis of titanium alkoxide precursors in the presence of nitrogen sources. Typical titanium salts (titanium tetrachloride) and alkoxide precursors (including titanium tetra-isopropoxide, tetrabutyl orthotitanate) have been used. Nitrogen containing precursors used include aliphatic amines, nitrates, ammonium salts, ammonia and urea. The synthesis route involves several steps; however, the main characteristic is that precursor hydrolysis is usually performed at room temperature. Pulverization and calcination were done to remove solvents from the precipitate at temperatures from 200 to 600 °C (Pelaez et al. 2012). The limitation of the slurry process is that the N- $\text{TiO}_2$  nanoparticles must be separated from the system after the treatment (Rashid et al. 2015; Vaiano et al., 2016). The use of magnetic core  $\text{TiO}_2$  nanoparticles offers a solution to this problem. The application of an external magnetic field to such materials provides an effortless way for removing and recycling the photocatalyst (Di Palma et al. 2015; Shirinova et al. 2016). In addition to incorporating an  $\text{SiO}_2$  intermediate layer between the  $\text{Fe}_3\text{O}_4$  (FM) core and the  $\text{TiO}_2$  shell weakens the adverse influence of  $\text{Fe}_3\text{O}_4$  on the photocatalysis of  $\text{TiO}_2$  (Rashid et al. 2015) and increase in its specific surface area by atomic mixing (Viet-Cuong and The-Vinh 2009). Magnetic photocatalyst obtained by coating  $\text{TiO}_2$  particles onto  $\text{Fe}_3\text{O}_4$  has been studied in the photocatalytic removal of phenols, the aim of this work was to obtain nanocomposites consisting of visible active N-doped  $\text{TiO}_2$  supported on  $\text{SiO}_2/\text{Fe}_3\text{O}_4$  ferromagnetic nanoparticles (N- $\text{TiO}_2/\text{FM}$ ) and to evaluate the performances and recyclability of N- $\text{TiO}_2/\text{FM}$  in the photocatalytic removal of phenol (Vaiano et al., 2016). Preparation of a magnetic photocatalyst by coating  $\text{TiO}_2$  particles onto iron oxide have been reported by Beydoun and co-workers. Due to its chemical inertia, silica ( $\text{SiO}_2$ ) has been proposed to be added between the magnetic particles core and  $\text{TiO}_2$  coating to overcome the above-mentioned problems. The application of an intermediate layer barrier such as  $\text{SiO}_2$  between the magnetic core and the titanium dioxide shell may lead to the avoidance of the photo dissolution of iron, magnetic core stabilization, and the prevention of the magnetic core from acting as an electron-hole recombination center which would negatively affect the photoactivity of  $\text{TiO}_2$ . The deposition of  $\text{TiO}_2$  onto silica-coated iron oxide has been conducted by several techniques such as impregnation, precipitation, and sol-gel (Hamzazadeh-Nakhjavani et al. 2015). The Spinning Disk Reactor (SDR) has many advantages when compared with other mixing devices used for precipitation process: i) a small liquid residence time, limiting the growth rate after nucleation, that leads to the production of narrow PDSs of nanoparticles at a specific target size; ii) micro-mixing conditions attained by means of a limited energy consumption; iii) continuous operation, compatible to industrial practice, can be performed (De Caprariis et al. 2015). The silica shell thickness can be controlled from 12.5 nm to 45 nm by varying the operating parameters. The reaction time, the ratio of TEOS/ $\text{Fe}_3\text{O}_4$ , and the concentration of hydrophilic  $\text{Fe}_3\text{O}_4$  seeds were found to be very important parameters in the control of silica shell thickness (Ruzmanova et al. 2013).

## 2. Materials and Methods

### 2.1 Synthesis of $\text{Fe}_3\text{O}_4$ - $\text{SiO}_2$ core-shell nanoparticles

The core-shell  $\text{SiO}_2/\text{Fe}_3\text{O}_4$  nanoparticles (FM) were prepared by two steps. Firstly,  $\text{Fe}_3\text{O}_4$  magnetic nanoparticles were synthesized using a spinning disk reactor. Then, FM nanoparticles were prepared by dispersing  $\text{Fe}_3\text{O}_4$  particles in distilled water, followed by the addition of  $\text{C}_2\text{H}_5\text{OH}$  (Sigma Aldrich). Tetraethyl ortosilicate (TEOS), preliminarily diluted in  $\text{C}_2\text{H}_5\text{OH}$ , was added drop-wise to the  $\text{Fe}_3\text{O}_4$  particle suspension. Then an aqueous solution of  $\text{NH}_3$  (30 wt %) was added and the TEOS hydrolysis and condensation was allowed under overnight gentle stirring. The obtained FM particles were washed in a centrifuge using firstly water/ethanol mixtures then distilled water. Finally, they were dried and calcinated at 450 °C for 30 minutes (Vaiano et al., 2016).

### 2.2 Synthesis of $\text{Fe}_3\text{O}_4$ - $\text{SiO}_2$ /N-doped $\text{TiO}_2$ nanoparticles

$\text{Fe}_3\text{O}_4$ - $\text{SiO}_2$ /N-doped  $\text{TiO}_2$  nanoparticles were prepared by adding urea in 50 ml water and continue the stirring for 10 minutes, then  $\text{Fe}/\text{SiO}_2$  was added in sonicator for 5 minutes finally TTIP was added under sonication followed by 10 minutes mechanical mixing. The mixture was centrifuged and washed two times. Finally, the recovered sample was calcinated at 450°C/30 minutes (Ramp 10°C/min) to obtain the final N- $\text{TiO}_2/\text{FM}$  catalyst. The nominal loading of N- $\text{TiO}_2$  on the FM support was 37.5 wt %.

## 2.3 Samples characterization

Physico-chemical samples characterization has been performed with different techniques. Laser Raman spectra were obtained at room temperature with a Dispersive Micro Raman (Invia, Renishaw), equipped with 514 nm laser, in the range 100-2500  $\text{cm}^{-1}$  Raman shift. UV-Vis reflectance spectra were recorded with a Perkin Elmer spectrometer Lambda 35. X-ray diffraction (XRD) was carried out using an X-ray micro-diffractometer Rigaku D-max-RAPID, using Cu-K $\alpha$  radiation and a cylindrical imaging plate detector. Diffraction data from 0 to 204 degree horizontally and from -45 to 45 degree vertically were collected. The average size and morphology of the nanoparticles was measured by SEM (FE-SEM HR Zeiss Auriga 405).

## 2.4 Photocatalysis tests

The photocatalytic experiments were carried out with initial concentration of phenol equal to 25  $\text{mg L}^{-1}$ , at room temperature (25°C). The catalyst dosage was 3  $\text{g L}^{-1}$ . The total volume of phenol aqueous solution was 80mL. The experiments were conducted using a pyrex cylindrical photoreactor (ID=2.5 cm, height=25 cm) equipped with an air distributor device ( $Q_{\text{air}}=150 \text{ cm}^3 \text{ min}^{-1}$  (STP)). Continuous mixing of the aqueous solution was done by external recirculation of the same solution using a peristaltic pump. The photoreactor was irradiated with a strip composed of 25 Blue light LEDs (6W nominal power; provided by New Orallight, with wavelength emission in the range 400–800 nm with main emission peak at 475 nm. The LEDs strip was positioned around and in contact with the external surface of the photoreactor (incident light intensity 32mW  $\text{cm}^{-2}$ ). The system was left in the dark for 30 min to reach phenol adsorption equilibrium, and then photocatalytic reaction was initiated under visible light for 180 min. The residual concentration of phenol in aqueous samples was monitored by observing the change in the absorbance at the maximum absorption wavelength of 270 nm using a UV-vis spectrophotometer (Lambda 35, Perkin Elmer), and then the concentration was calculated from a calibration curve.

## 3. Results and Discussion

### 3.1 Samples characterization

Crystal phase composition and of N-TiO<sub>2</sub>, FM and N-TiO<sub>2</sub>/FM was determined by XRD and RAMAN. The XRD and RAMAN spectra are reported in Figure 1.

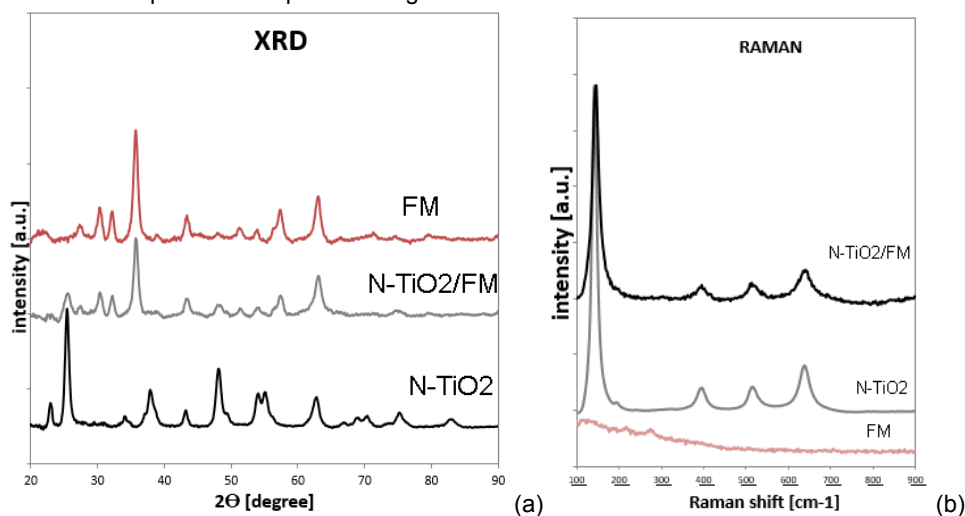


Figure 1: Catalysts XRD spectra (a) N-TiO<sub>2</sub>, FM and N-TiO<sub>2</sub>/FM and Raman spectra (b) N-TiO<sub>2</sub>, FM and N-TiO<sub>2</sub>/FM

XRD result of FM sample exhibited the presence of the the orthorhombic phase of Fe<sub>3</sub>O<sub>4</sub> (Vaiano et al., 2016). From the analysis of XRD spectra of N-TiO<sub>2</sub>/FM compared with those of FM and unsupported N-TiO<sub>2</sub> powder, it was found the presence of the anatase-TiO<sub>2</sub> peaks with together the signals of FM. The same composition and structure was confirmed by Raman analysis (Figure 1b). Anatase and Fe<sub>3</sub>O<sub>4</sub> crystallite size of the samples were evaluated from XRD analysis, using the Scherrer equation. For N-TiO<sub>2</sub>, the anatase crystallite size was about 11 nm and slightly decreased (8 nm) after the deposition of N-TiO<sub>2</sub> on FM. Fe<sub>3</sub>O<sub>4</sub> particle size was found to be about 20 - 30 nm which corresponds to the determined average particle size by SEM measurement (Figures 2a and 2b).

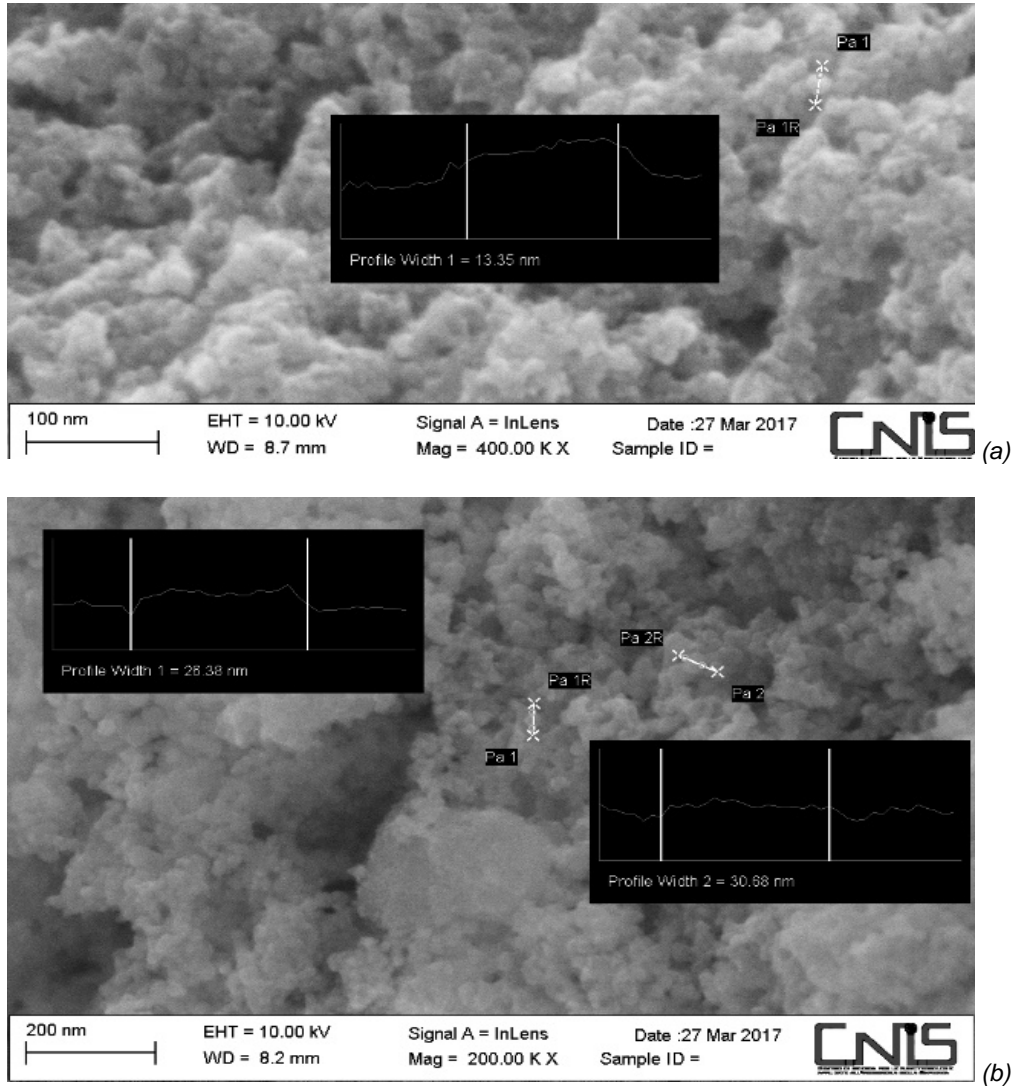


Figure 2: N-TiO<sub>2</sub> SEM (a) and N-TiO<sub>2</sub>/FM SEM (b).

Figure 3a reports the UV-vis reflectance spectra in terms of Reflectance for N-TiO<sub>2</sub>. The shifting of the absorption onset from about 350 nm (for undoped TiO<sub>2</sub>) to about 550 nm (for N-TiO<sub>2</sub>) indicates the ability of the sample to absorb visible light, as confirmed by the results in Figure 3b, which is the typical absorption property of TiO<sub>2</sub> doped with nitrogen (Vaiano et al., 2016). Composition of elements in N-TiO<sub>2</sub> and N-TiO<sub>2</sub>/FM were checked by EDX- SEM characterization, reported in Figure 4.

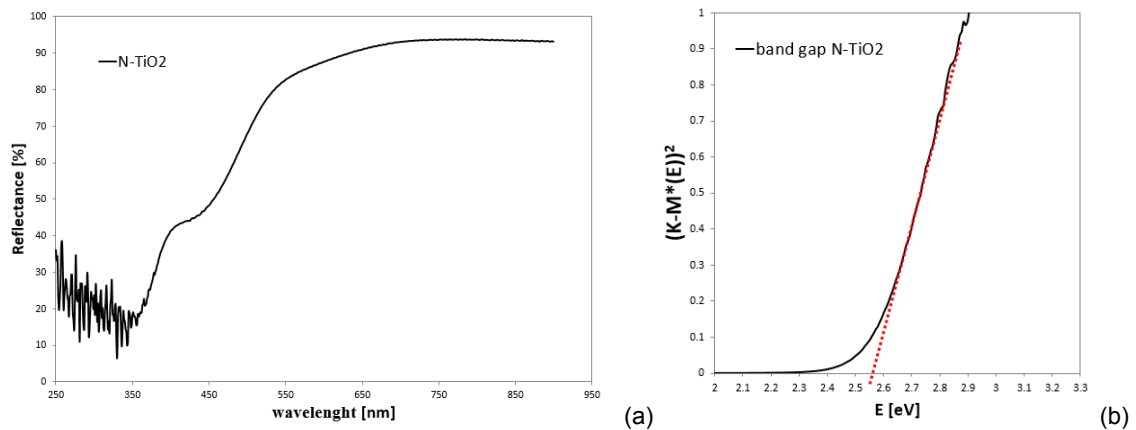


Figure 3: N-TiO<sub>2</sub> UV-Vis DRS-Spectra (a) and N-TiO<sub>2</sub> UV-DRS (band gap) (b)

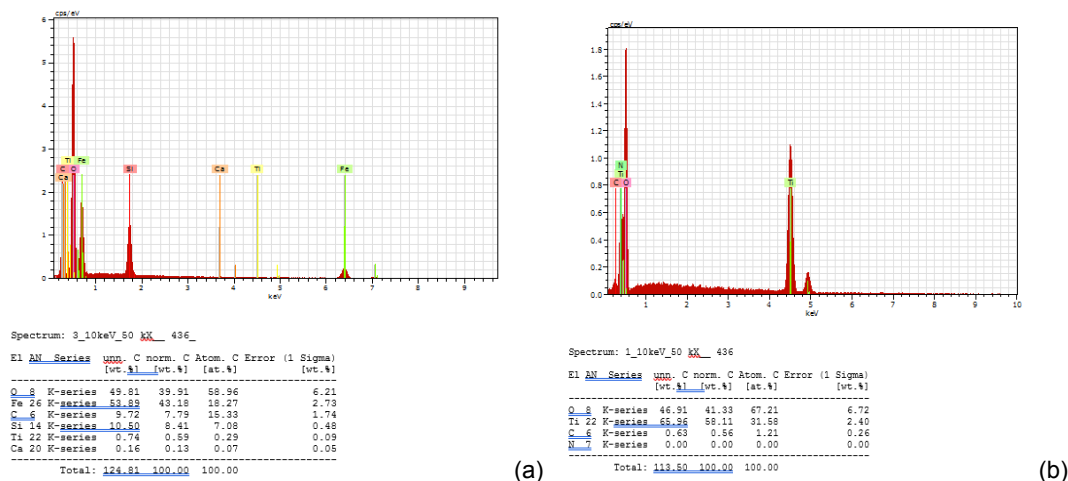


Figure 4: N-TiO<sub>2</sub> EDX (a) and Fe/SiO<sub>2</sub>/N-TiO<sub>2</sub> EDX (b).

### 3.2 Photocatalytic activity results

Preliminary experiments were carried out to verify that phenol was removed by the heterogeneous photocatalytic process under visible light. It was found that in the absence of photocatalyst, no decrease in phenol concentration was observed (Vaiano et al., 2016). Therefore, photolysis phenomena did not occur. Figure 5a reports the photocatalytic activity of N-TiO<sub>2</sub> and N-TiO<sub>2</sub>/FM.

After 180 min of visible light irradiation, no photocatalytic activity was observed for FM sample (Vaiano et al., 2016). On the contrary, both N-TiO<sub>2</sub> and N-TiO<sub>2</sub>/FM catalysts were effective in the degradation of phenol in aqueous solutions. The degradation efficiency of N-TiO<sub>2</sub> and N-TiO<sub>2</sub>/FM were 55% and 76%, respectively. These values are higher than those reported by other researchers, concerning the photocatalytic degradation of phenol under visible light irradiation (Vaiano et al., 2016). The higher photocatalytic activity of N-TiO<sub>2</sub>/FM compared to N-TiO<sub>2</sub> particles could be attributed to the lower anatase crystallite size obtained with N-TiO<sub>2</sub>/FM sample. As the separability of photocatalysts from treated wastewater in a practical wastewater treatment system is very important, magnetic N-TiO<sub>2</sub>/FM sample was chosen for investigating the stability and efficiency after four reuse cycles (Figure 5b). The treated water containing N-TiO<sub>2</sub>/FM catalyst was collected into a beaker after each test cycle and the use of a magnet on the external surface of the beaker allows to easily separate the treated solution from the used photocatalyst. After washing with distilled water and drying at 100°C, the photocatalyst was reused without further treatment. Photocatalytic tests on the recycled catalyst showed that, after four reuse cycles, N-TiO<sub>2</sub>/FM catalyst remained stable, evidencing phenol degradation in the range 71-76 %.

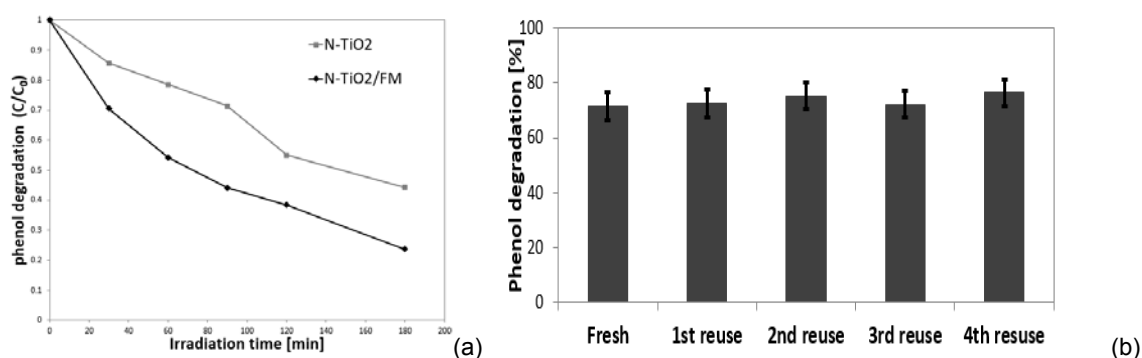


Figure 5: Phenol photodegradation (a) N-TiO<sub>2</sub> and N-TiO<sub>2</sub>/FM and reusability and efficiency of catalysts (b) N-TiO<sub>2</sub>/FM

### 4. Conclusions

Nanocomposite N-TiO<sub>2</sub>/SiO<sub>2</sub>/Fe<sub>3</sub>O<sub>4</sub> (N-TiO<sub>2</sub>/FM), which are visible-active and magnetically separable, was synthesized successfully and tested in the photocatalytic removal of phenol under visible light irradiation. The XRD and Raman results confirmed the presence of crystalline magnetite, SiO<sub>2</sub>, and TiO<sub>2</sub> in anatase phase

and the average nanoparticle size of N-TiO<sub>2</sub>/FM magnetic core was about 26 nm, and composition was successfully checked by SEM-EDX. The photocatalytic tests were carried out in a recirculating batch cylindrical photoreactor irradiated by a strip of white LEDs surrounding the external surface of the reactor and emitting in the visible region. After an irradiation time of 180 min, the experimental results showed that N-TiO<sub>2</sub>/FM nanoparticles are effective in the removal of phenol, reaching a value of 76%. The results of visible active magnetic catalyst reuse showed the effectiveness of prepared samples after four cycles of repetitive use, evidencing phenol degradation in the range 71-76%.

## Reference

- Asahi, R. Morikawa T., Ohwaki T., Aoki K., Taga Y., 2001. Visible-Light Photocatalysis in Nitrogen-Doped Titanium Oxides. *Science*, 293(5528), pp.269–271.
- Bavasso I., Vilardi G., Stoller M., Chianese A., Di Palma L., 2016. Perspectives in nanotechnology based innovative applications for the environment. *Chemical Engineering Transactions*, 47, 55-60. doi: 10.3303/CET1647010.
- Beydoun, D., Amal R., Low G. K. C., McEvoy S., 2000. Novel Photocatalyst: Titania-Coated Magnetite. Activity and Photodissolution. *The Journal of Physical Chemistry B*, 104(18), pp.4387–4396.
- Choquette-Labbé, M., Shewa, W., Lalman, J., & Shanmugam, S. (2014). Photocatalytic Degradation of Phenol and Phenol Derivatives Using a Nano-TiO<sub>2</sub> Catalyst: Integrating Quantitative and Qualitative Factors Using Response Surface Methodology. *Water*, 6(6), 1785–1806. <https://doi.org/10.3390/w6061785>.
- De Caprariis B., Stoller M., Chianese A., Verdone N., 2015. Cfd model of a spinning disk reactor for nanoparticle production. *Chemical Engineering Transactions*, 43, 757-762.
- Di Palma, L., Medici, F. Vilardi, G., 2015. Artificial aggregate from non-metallic automotive shredder residue. *Chemical Engineering Transactions*, 43, pp.1723–1728.
- Fujishima, A., Honda, K., 1972. TiO<sub>2</sub> photoelectrochemistry and photocatalysis. *Nature*, 213(1998), p.8656.
- Hamzezadeh-Nakhjavani, S. Tavakoli O., Akhlaghi S. P., Salehi Z., Esmailnejad-Ahranjani P., Arpanaei A., 2015. Efficient photocatalytic degradation of organic pollutants by magnetically recoverable nitrogen-doped TiO<sub>2</sub> nanocomposite photocatalysts under visible light irradiation. *Environmental Science and Pollution Research*, 22(23), pp.18859–18873.
- Muradova G. G., Gadjeva S. R., Di Palma L., Vilardi, G., 2016. Nitrates Removal by Bimetallic Nanoparticles in Water. *Chemical Engineering Transactions*, 47, 205-210. doi: 10.3303/CET1647035.
- Pelaez, M., et al., 2012. A review on the visible light active titanium dioxide photocatalysts for environmental applications. *Applied Catalysis B: Environmental*, 125, pp.331–349.
- Rashid, J., Barakat M. A., Ruzmanova Y., Chianese, A. 2015. Fe<sub>3</sub>O<sub>4</sub>/SiO<sub>2</sub>/TiO<sub>2</sub> nanoparticles for photocatalytic degradation of 2-chlorophenol in simulated wastewater. *Environmental Science and Pollution Research*, 22(4), pp.3149–3157.
- Ruzmanova, Y., Ustundas M., Stoller M., Chianese, A., 2013. Photocatalytic Treatment of Olive Mill Wastewater by N-doped Titanium Dioxide Nanoparticles under Visible Light. *Chemical Engineering Transactions*, 32, 2233-2238.
- Ruzmanova Y., Stoller M., Bravi M., Chianese A., 2015, A novel approach for the production of nitrogen doped tio<sub>2</sub> nanoparticles, *Chemical Engineering Transactions*, 43, 721-726 DOI: 10.3303/CET1543121.
- Shawabkeh, R.A., Khashman, O.A. Bisharat, G.I., 2010. Photocatalytic Degradation of Phenol using Fe-TiO<sub>2</sub> by Different Illumination Sources. *International Journal of Chemistry*, 2(2), p.10.
- Shirinova H., Di Palma L., Sarasini F., Tirillo J., Ramazanov M., Hajiyeva F., Sannino D., Polichetti M., Galluzzi A., 2016. Synthesis and characterization of magnetic nanocomposites for environmental remediation. *Chemical Engineering Transactions*, 47, 103-108.
- Stoller M., Azizova G., Mammadova A., Vilardi G., Di Palma L., Chianese A., 2016. Treatment of Olive Oil Processing Wastewater by Ultrafiltration, Nanofiltration, Reverse Osmosis and Biofiltration. *Chemical Engineering Transactions*, 47, 409-414. doi: 10.3303/CET1647069.
- Vaiano V., Sacco O., Sannino D., Stoller M., Ciambelli P., Chianese A., 2016, Photocatalytic removal of phenol by ferromagnetic n-tio<sub>2</sub>/sio<sub>2</sub>/fe<sub>3</sub>o<sub>4</sub> nanoparticles in presence of visible light irradiation, *Chemical Engineering Transactions*, 47, 235-240.
- Viet-Cuong, N., The-Vinh, N., 2009. Photocatalytic decomposition of phenol over N-TiO<sub>2</sub>-SiO<sub>2</sub> catalyst under natural sunlight. *Journal of Experimental Nanoscience*, 4(3), pp.233–242.
- Vilardi G., Di Palma L., 2017. Kinetic Study of Nitrate Removal from Aqueous Solutions Using Copper-Coated Iron Nanoparticles. *Bulletin of Environmental Contamination and Toxicology*, 98(3), pp.359–365. doi:10.1007/s00128-016-1865-9.
- Vilardi G., Verdone N., Di Palma L., 2017. The influence of nitrate on the reduction of hexavalent chromium by Zero Valent Iron nanoparticles in polluted wastewater. *Desalination and Water Treatment*, In Press.